Statics and dynamics of the ten-state mean-field Potts glass model: a Monte Carlo study

2002 J. Phys. A: Math. Gen. 35 191

(http://iopscience.iop.org/0305-4470/35/2/302)

INSTITUTE OF PHYSICS PUBLISHING JOURNAL OF PHYSICS A: MATHEMATICAL AND GENERAL

J. Phys. A: Math. Gen. **35** (2002) 191–216 PII: S0305-4470(02)25932-6

Statics and dynamics of the ten-state mean-field Potts glass model: a Monte Carlo study

Claudio Brangian, Walter Kob[1,2] and Kurt Binder

Institut für Physik, Johannes Gutenberg Universität Mainz, D-55099 Mainz, Staudinger Weg 7, Germany

Received 18 June 2001, in final form 3 September 2001
Published 4 January 2002
Online at stacks.iop.org/JPhysA/35/191

Abstract

We investigate by means of Monte Carlo simulations the fully connected p-state Potts model for different system sizes in order to see how the static and dynamic properties of a finite model compare with the, exactly known, behaviour of the system in the thermodynamic limit. Using $p = 10$ we are able to study the equilibrium dynamics for system sizes as large as $N = 2560$. We find that the static quantities, such as the energy, the entropy, the spin glass susceptibility as well as the distribution of the order parameter $P(q)$ show very strong finite-size effects. From $P(q)$ we calculate the fourth-order cumulant $g_4(N, T)$ and the Guerra parameter $G(N, T)$ and show that these quantities cannot be used to locate the static transition temperature for the system sizes investigated. Also the spin-autocorrelation function $C(t)$ shows strong finite-size effects in that it does not show a plateau even for temperatures around the dynamical critical temperature T_D. We show that the dependence on N and T of the α-relaxation time can be understood by means of a dynamical finite-size scaling ansatz. $C(t)$ does not obey the time–temperature superposition principle for temperatures around T_D, but does so for significantly lower T. Finally we study the relaxation dynamics of the individual spins and show that their dependence on time depends strongly on the chosen spin, i.e. that the system is dynamically very heterogeneous, which explains the non-exponentiality of $C(t)$.

PACS numbers: 05.50.+q, 05.10.Ln, 75.10.-b

1. Introduction

In recent years it has been recognized that the relaxation dynamics of supercooled liquids and that of spin glass systems have many properties in common [1–4]. Of particular significance was the observation by Kirkpatrick *et al* [5] that for certain mean-field spin glasses the equations

[1] Author to whom any correspondence should be addressed.
[2] Present and permanent address: Laboratoire des Verres, Université Montpellier II, 34095 Montpellier, France.

of motion for the spin-autocorrelation function $C(t)$ are formally the same as the ones that have been derived previously for the relaxation of particle-density-correlation functions of structural glasses [6]. That result thus opened the possibility to find one common description for these two classes of glassy systems: the spin glasses with quenched disorder and the structural glasses in which the disorder is not included explicitly in the Hamiltonian.

One of the important classes of spin glass models is the Potts glass [5, 7–19], which is a generalization of the Ising spin glass [20–27], where the spins σ_i can assume two values ($\sigma_i = \pm 1$), to the case where each Potts 'spin' can be in one of p discrete states, $\sigma_i \in \{1, 2, \ldots, p\}$, p being an integer. Just as the Potts ferromagnet [28–30] is a 'workhorse' for the statistical mechanics of phase transitions, since it has served to test many methods and to exemplify many concepts about the subject, one can expect the Potts glass to play a similar role for the study of the glass transition in systems with quenched disorder or the properties of liquids close to their glass transition temperature, since the possibility of changing p allows one to describe different glass transition scenarios, e.g. from a continuous transition to a discontinuous one.

It is important to note that in the Potts glass it is well established that for $p > 4$ one has both a *dynamical* transition at a temperature T_D, where the relaxation time associated with $C(t)$ diverges, and a *static* transition at a temperature $T_0 < T_D$, where a glass order parameter appears discontinuously, accompanied by a kink in the entropy (as well as in the internal energy). In contrast to this known feature, for the structural glass transition the existence of an underlying static transition, although proposed a long time ago [31, 32], is still an open question [33–38]. Thus a study of Potts glasses should help us also to better understand structural glasses and hence is a welcome addition to the great efforts made to identify which structural features distinguish the solid glass from the liquid from which it was formed [6, 33–41].

Besides this interest in the Potts glass as a possible prototype model for the structural glass transition, it can also be considered as a coarse-grained model for orientational glasses [42–44]. Experimentally, these systems are created by random dilution of molecular crystals, which has the effect that at low temperatures the quadrupole moments of the molecules freeze in random orientations [42]. If the crystal anisotropy singles out p discrete preferred orientations (e.g. the four diagonal directions in a cubic crystal), a Potts glass model with p states may give a qualitatively correct description of the system. And, last but not least, the Potts glass model of course completes our knowledge about the different types of phase transition and ordered phase that spin glasses can exhibit [22–27], which provides an additional motivation for the great activity in this field [5, 7–19],

In this work, we use Monte Carlo simulations to study the Potts glass model. Our goal is to clarify to what extent this interesting and non-trivial mean-field behaviour which is known exactly in the thermodynamic limit, $N \to \infty$, can be seen for *finite* N. In addition, we want to elucidate the dynamical behaviour of the model in greater detail than has been done so far and thus help to clarify the reasons for non-Debye relaxation in glassy systems.

In the present paper, we shall first define the model and introduce the quantities that will be investigated (section 2). In section 3 we summarize what is known about the static behaviour of the model and describe our pertinent numerical results. Section 4 is then devoted to the dynamical properties in the high-temperature phase, i.e. above T_D, and the finite-size behaviour at T_D, while section 5 is concerned with the dynamical behaviour of small systems in the low-temperature phase. By following the relaxation of individual spins we are able to also study the 'dynamical heterogeneities' [45, 46] at low temperatures. Finally, section 6 summarizes our conclusions.

2. Model and simulation methods

In this section we define the Hamiltonian and the observables that we consider in this work. Subsequently we give the details of the simulations.

The Hamiltonian of the p-state mean-field Potts glass of N interacting Potts spins σ_i ($i = 1, 2, \ldots, N$) that can take p discrete values $\sigma_i \in \{1, 2, \ldots, p\}$ is defined as

$$\mathcal{H} = -\sum_{i<j} J_{ij}(p\delta_{\sigma_i\sigma_j} - 1). \tag{1}$$

The 'exchange constants' (bonds) J_{ij} are quenched random variables which we assume to be distributed according to a Gaussian distribution $P(J_{ij})$:

$$P(J_{ij}) = \frac{1}{\sqrt{2\pi}(\Delta J)} \exp\left[-\frac{(J_{ij} - J_0)^2}{2(\Delta J)^2} \right]. \tag{2}$$

The first two moments J_0 and ΔJ are chosen as follows:

$$J_0 \equiv \left[J_{ij}\right]_{av} = \tilde{J}_0/(N-1) \qquad \tilde{J}_0 = 3 - p \tag{3}$$

$$(\Delta J)^2 \equiv \left[J_{ij}^2\right]_{av} - \left[J_{ij}\right]_{av}^2 = 1/(N-1) \tag{4}$$

where $[\cdots]_{av}$ denotes an average over all realizations of disordered bonds (while thermal equilibrium averages will be denoted as $\langle\cdots\rangle$). The scaling of the parameters J_0, ΔJ with N was chosen such as to ensure a sensible thermodynamic limit both for the spin glass transition and for the ferromagnetic transition (which occurs for a certain range of values of $\tilde{J}_0$). Note that for $p = 2$ equations (1)–(4) simply reduce to the Sherrington–Kirkpatrick (SK) model of a spin glass [21]. We also mention that the term $\sum_{i<j} J_{ij}$ in equation (1) is only included for convenience, since it makes the mean energy of *each system*, i.e. for each realization of the disorder, go to zero for $T \to \infty$. For the present choice of the parameter ΔJ, the spin glass transition in the replica-symmetric approximation, within which one finds a second-order transition for $p < 6$, occurs at a temperature $T_s = 1$ [7]. (Here and in the following we set Boltzmann's constant $k_B \equiv 1$.) While for some choices of $\tilde{J}_0$ the system exhibits a transition to a standard ferromagnetic phase at a temperature $T_F > T_s$, for our choice of parameters T_F falls far below T_s and hence ferromagnetic order is of no of interest here [7, 11].

There exists in addition a second transition to a different type of spin glass phase (sometimes called a 'randomly canted ferromagnetic phase') [7, 9], at a transition temperature T_2 which is given by

$$T_2 = (p/2 - 1)/(1 - \tilde{J}_0). \tag{5}$$

For the choice of $\tilde{J}_0$ given in equation (3) one thus finds $T_2 = 1/2$. Hence this choice ensures that at the temperatures of interest in the present study, $T \geqslant 0.7$, any effect of this second transition on physical observables should be negligible.

For defining observables like the magnetization, the glass order parameter, and time-dependent spin-autocorrelation functions etc, it is useful to choose a representation for the spins that takes into account the symmetry between their p possible states. This can be achieved by the so-called 'simplex representation' [29, 30] in which the p states correspond to $(p-1)$-dimensional vectors $\vec{S}_\lambda$ pointing towards the corners of a p-simplex, i.e.

$$\vec{S}_\lambda \cdot \vec{S}_{\lambda'} = (p\delta_{\lambda\lambda'} - 1) \qquad \text{with } \lambda, \lambda' = 1, \ldots, p. \tag{6}$$

In our study we consider static as well as dynamical observables. Static quantities include the energy per spin,

$$e = [\langle\mathcal{H}\rangle]_{av}/N \tag{7}$$

and the spin glass susceptibility χ_{SG}, and also the spin glass order parameter distribution function $P(q)$. For defining a spin glass order parameter, we follow the standard method used for Potts glasses [12,16,19] to consider two replicas α and β of the system, i.e. two systems that have identical bond configurations, and to carry out for each of them an independent Monte Carlo simulation. The order parameter tensor is then defined as

$$q^{\mu\nu} = \frac{1}{N}\sum_{i=1}^{N}(\vec{S}_{i,\alpha})^{\mu}(\vec{S}_{i,\beta})^{\nu} \qquad \mu, \nu = 1, 2, \ldots, p-1. \tag{8}$$

In an equilibrium simulation of a finite system with no external fields that couple to odd moments of the order parameter, the symmetry is not broken. Hence it is useful to consider the root mean square order parameter q defined as [5, 12, 16, 19]

$$q = \left[\frac{1}{p-1}\sum_{\mu,\nu=1}^{p-1}(q^{\mu\nu})^2\right]^{1/2} \tag{9}$$

and by calculating a histogram of q, i.e. by taking first the thermal average and then the average over the disorder, one can estimate the above-mentioned distribution $P(q)$. The second moment of this distribution is related to the *reduced* spin glass susceptibility $\tilde{\chi}_{SG}$:

$$\tilde{\chi}_{SG} = \frac{N}{p-1}[\langle q^2\rangle]_{av} = \frac{N}{p-1}\int_0^1 q^2 P(q)\,\mathrm{d}q. \tag{10}$$

(Below we will discuss the relation between $\tilde{\chi}_{SG}$ and the *standard* spin glass susceptibility χ_{SG}; see equations (21) and (26).) If there is a second-order transition to a spin glass phase, $\tilde{\chi}_{SG}$ should show a divergence at the critical temperature. Further interesting quantities related to the distribution $P(q)$ are the reduced fourth-order cumulant [12, 16, 19]

$$g_4(N,T) = \frac{(p-1)^2}{2}\left(1 + \frac{2}{(p-1)^2} - \frac{[\langle q^4\rangle]_{av}}{[\langle q^2\rangle]_{av}^2}\right) \tag{11}$$

and a quantity called the Guerra parameter [47]

$$G(N,T) = \frac{[\langle q^2\rangle^2]_{av} - [\langle q^2\rangle]_{av}^2}{[\langle q^4\rangle]_{av} - [\langle q^2\rangle]_{av}^2}. \tag{12}$$

The reason for introducing these ratios of moment is that they are useful in the context of finite-size scaling analysis of phase transitions. They are defined such that for $N = \infty$ they are zero in the disordered phase and non-zero in the ordered phase. In the finite-size scaling limit the curves $g_4(T)$, or $G(T)$, for different system sizes N should intersect in a common point at the static phase transition point. In particular, G is a measure for the lack of self-averaging.

To study the dynamical properties of the system, we will mainly focus on the autocorrelation function of the Potts spins:

$$C(t) = \frac{1}{N(p-1)}\sum_{i=1}^{N}[\langle \vec{S}_i(t') \cdot \vec{S}_i(t'+t)\rangle]_{av}. \tag{13}$$

Note that in thermal equilibrium $C(t)$ depends only on the time difference t, i.e. it is independent of the second argument t' occurring on the right-hand side of equation (13). In practice, for the Monte Carlo sampling using the Metropolis algorithm [48], the thermal averaging $\langle\cdots\rangle$ is a time averaging over the initial times t'.

We have also considered a rotationally invariant order parameter time-displaced correlation function $C_{RI}(t)$ which is defined as

$$C_{RI}(t) = \left[\frac{\langle\tilde{q}(t)\rangle}{\langle\tilde{q}(0)\rangle}\right]_{av} \tag{14}$$

with

$$\tilde{q}(t) = \left[\frac{1}{p-1} \sum_{\mu,\nu=1}^{p-1} (\tilde{q}^{\mu\nu}(t))^2 \right]^{1/2} \qquad \text{and} \qquad \tilde{q}^{\mu\nu}(t) = \frac{1}{N} \sum_{i=1}^{N} (\vec{S}_i)^{\mu}(t)(\vec{S}_i)^{\nu}(0). \tag{15}$$

Note that $\tilde{q}^{\mu\nu}$ is not the same quantity as $q^{\mu\nu}$ defined in equation (8), since the latter involves two replicas α and β. However, for $t \to \infty$ the thermodynamic averages of the two quantities are the same. This means that in this limit also $\tilde{q}$ and q, from equation (9), are the same. Furthermore, we mention that the expectation value $\langle \tilde{q}(0) \rangle$ occurring in equation (14) is equal to 1, as long as there is no ferromagnetic ordering of the system. It is important to realize that $C_{RI}(t \to \infty)$ is not zero, if N is finite. This follows immediately from equation (15), since for large t the quantity $\tilde{q}^{\mu\nu}(t)$ is of order $1/\sqrt{N}$, and $\tilde{q}(t)$, as a finite sum over the square of such quantities, is hence positive and also of order $1/\sqrt{N}$. From equation (10) one also concludes that $C_{RI}(t \to \infty)$ is of order $\sqrt{\tilde{\chi}_{SG}/N}$.

In our simulations, we have investigated five different system sizes, $N = 160$, 320, 640, 1280 and 2560. The number of samples used to approximate the quenched average $[\cdots]_{av}$ over the bond disorder was 500 for $N = 160$, 200 for $N = 320$, 100 for $N = 640$ and 1280 and between 20 and 50 for $N = 2560$ (depending on temperature). At not-too-low temperatures, $T \geqslant 1$, the straightforward Metropolis algorithm was implemented [48], picking spins at random and choosing randomly an orientation for them as a trial configuration. Depending on the energy difference ΔE between the old configuration and the trial configuration, the trial configuration was always accepted if $\Delta E \leqslant 0$, else it was accepted with probability $P = \exp(-\Delta E/T)$. For temperatures $T < 1$ the equilibrium configurations were generated with the 'parallel tempering' technique [49–51]. These equilibrium configurations can both be used to study the static properties of the model and as starting configurations to study the usual Metropolis dynamics in equilibrium and thus to calculate $C(t)$, although at very low temperatures the relaxation is so slow that one cannot follow the complete decay of $C(t)$ to zero. The total computing time (in units of a single Pentium II processor with 400 MHz) used for this study was of the order of 10 years.

3. Static properties of the ten-state Potts glass model

In this section we first discuss the analytic results for the static properties of the model in the thermodynamic limit. Subsequently we compare them with the results of the simulations for finite N.

If one calculates the free energy of the model given by equations (1)–(4) with the replica method [20–27], (without allowing for replica-symmetry breaking), one obtains, depending on the value of $\tilde{J}_0$ but independently of p, either a transition to a spin glass phase (where the spin glass order parameter q_0 is non-zero) or to a ferromagnet (with a spontaneous magnetization m_0). Within this approach and close to a critical temperature T_s the free-energy density $f(q_0, m_0)$ can be written as follows [7]:

$$-f(q_0, m_0)/T = \frac{1}{2} r' \left(1 - \frac{T_s}{T}\right) q_0^2 + \frac{1}{6} u q_0^3 + \frac{1}{2} r_m m_0^2 + \frac{1}{6} u_m m_0^4 + \frac{1}{6} u' q_0^2 m_0^2 + \cdots \tag{16}$$

where with our choice of units $T_s = 1$, and r', u, r_m, u_m, u' are constants that are of no interest to us here. If the parameters are chosen such that the transition that occurs at T_s is to a spin glass phase, it is found that the order parameter distribution $P(q)$ is a δ-function whose position depends on T (we consider here only the case $u > 0$):

$$P(q) = \delta(q) \qquad \text{for } T > T_s \tag{17}$$

$$P(q) = \delta(q - q_0) \qquad \text{with } q_0 = \frac{2r'}{u}\left(\frac{T_s}{T} - 1\right) \qquad \text{for } T < T_s. \tag{18}$$

Note that the first term on the right-hand side of equation (16) can also be interpreted in terms of the spin glass susceptibility[3] χ_{SG} as $\frac{1}{4}\chi_{SG}^{-1}q_0^2$. Thus close to T_s one finds for χ_{SG} a Curie–Weiss law:

$$\chi_{SG} = \left[2r'(1 - T_s/T)\right]^{-1} \qquad T > T_s. \tag{19}$$

The coefficient r' in equation (16) is given by [7] (a result coming from the expansion in q of the free energy close to T_s)

$$r' = \frac{p-1}{2}\left(\frac{T_s}{T}\right)^2\left(1 + \frac{T_s}{T}\right). \tag{20}$$

We thus find for the susceptibility χ_{SG} around T_s (remember that $T_s = 1$ in our normalization)

$$\chi_{SG}^{-1} = 2(p-1)\left(1 - \frac{T_s}{T}\right) \qquad T \approx T_s. \tag{21}$$

The difference between the standard spin glass susceptibility and the reduced one defined in equation (10) is just the factor $(p-1)$, related to the susceptibility of a system of non-interacting spins.

It is well known [5,9,11] that, if one allows for replica-symmetry breaking, the prediction that there is a second-order transition to a spin glass phase remains valid only if $p \leqslant 4$. For $p > 4$, a new type of first-order transition to a glass phase is predicted to occur at a temperature T_0 which is higher than T_s. Although at T_0 the order parameter jumps discontinuously from zero to a value $q_0 > 0$, there is no latent heat involved in this transition. Instead of equation (18) the order parameter distribution acquires now a double-δ-function structure [5,9,11]:

$$P(q) = [1 - w(T)]\delta(q) + w(T)\delta(q - q_0(T)) \qquad T < T_0 \tag{22}$$

with $w(T) = 1 - T/T_0$ for $T \to T_0^-$. While it is possible to calculate q_0 and T_0 analytically for $p \to 4^+$ (see e.g. [11]):

$$q_0 = \tfrac{2}{7}(p-4) + \mathrm{o}(p-4)^2 \qquad T_0 - T_s \propto (p-4)^2 + \mathrm{o}(p-4)^3 \tag{23}$$

for integer $p > 4$ the correct values for q_0 and T_0 can be obtained only numerically [13]. For example, for our case of $p = 10$ the predicted values are

$$T_0 = 1.1312 \qquad \text{and} \qquad q_0(T_0) = 0.452. \tag{24}$$

In the disordered phase, the internal energy per spin e and entropy per spin s are given by [7,13]

$$e = -\frac{p-1}{2}\frac{T_s}{T} \qquad s = \ln p - \frac{p-1}{4}\left(\frac{T_s}{T}\right)^2. \tag{25}$$

and a high-temperature expansion gives [24]

$$\tilde{\chi}_{SG}^{-1} = \left[1 - \left(\frac{T_s}{T}\right)^2\right] \qquad T > T_0. \tag{26}$$

Within the replica-symmetric ansatz these expressions are correct for $T > T_s$. If one allows for replica-symmetry breaking they hold only for $T > T_0$. Although no *explicit* analytic expressions for $e(T)$ and $s(T)$ are known for $T < T_0$, their values can be calculated numerically [13].

Finally we mention that within the replica ansatz (symmetric or broken), neither T_s nor T_0 depend on the choice of $\tilde{J}_0$ from equation (3), provided that the temperature T_F of the transition

[3] For the definition of a proper conjugate field to define the spin glass susceptibility, see [22, 62].

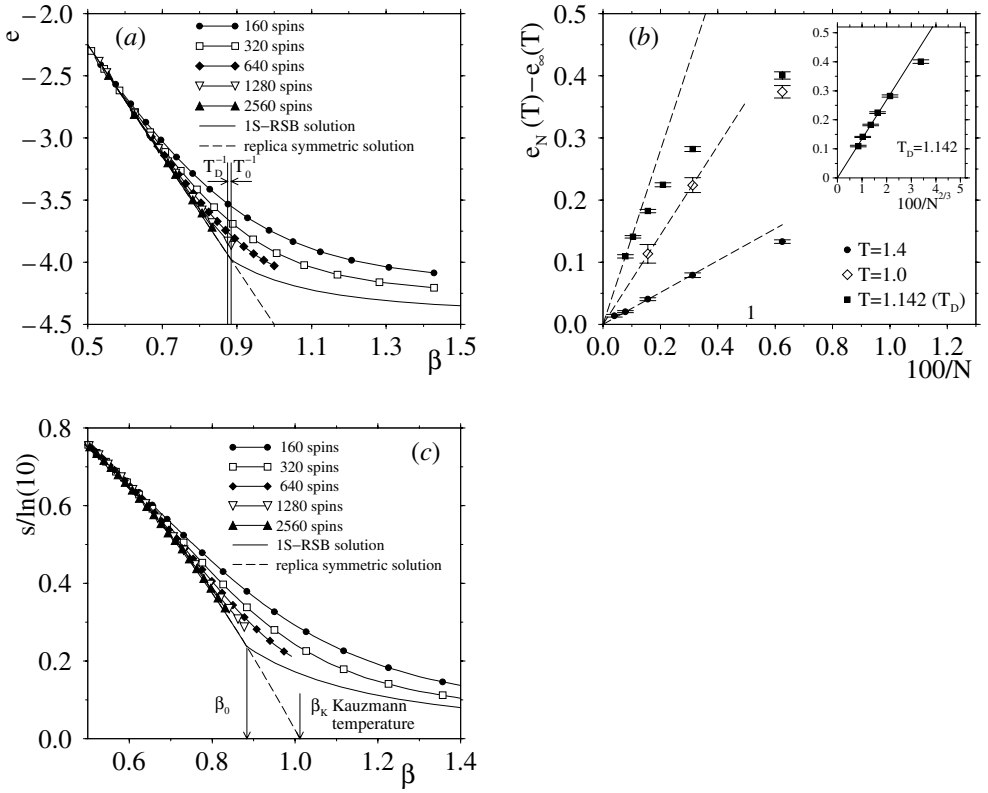

Figure 1. (*a*) Energy e per spin plotted versus inverse temperature $\beta = 1/T$ for different system sizes (curves with symbols). The bold solid curve shows the one-step replica-symmetry-breaking solution of De Santis *et al* [13, 53], the broken curve—which coincides with the former for $T \geqslant T_0$—is the replica-symmetric solution, equation (25). The thin vertical lines indicate the inverse temperatures β_D (left) and β_0 (right) of the dynamical transition and the static transition, respectively. (*b*) Analysis of the size dependence of the energy difference $e_N(T) - e_\infty(T)$, using the one-step replica-symmetric solution of De Santis *et al* [13] to calculate $e_\infty(T)$. The inset shows the data for $T = T_D = 1.142$ plotted versus $N^{-2/3}$ instead of N^{-1}. (*c*) Entropy s per spin, normalized by its high-temperature value, plotted versus inverse temperature for different system sizes (curves with symbols). The bold dashed curve and the bold solid curve are the replica-symmetric solution and the one-step replica-symmetry-breaking solution, respectively. Vertical arrows indicate the static inverse transition temperature β_0 and the inverse of the 'Kauzmann temperature' β_K, where the entropy of the replica-symmetric solution vanishes.

from the disordered phase to the collinear ferromagnetic phase, discussed in section 2, is not above T_0 [7, 11]. T_F is given by the following equation, for arbitrary p [7]:

$$T_F^{-1} = \frac{\tilde{J}_0}{(p-2)} \left[-1 + \sqrt{1 + 2(p-2)/\tilde{J}_0^2} \right]. \tag{27}$$

De Santis *et al* [13] used $\tilde{J}_0 = \frac{1}{2}(4-p)$ in which case $T_F = T_s = 1$, independently of p. However, this case is rather special since then the temperature T_2 of the transition to the randomly canted ferromagnetic phase, discussed in the introduction, coincides with $T_s = 1$, as can be seen from equation (5). For our choice of $\tilde{J}_0 = 3 - p$ we have instead $T_2 = 1/2$ for all p and $T_F = 8/(7-\sqrt{65}) \approx 0.531$ for $p = 10$. Thus with this choice we hence make sure that the ferromagnetic fluctuations are still very small at $T_s = 1$, even if the system size is rather small.

We now present our numerical results and compare them to the analytical predictions that we just discussed. Figure 1(*a*) shows a plot of the internal energy versus inverse temperature, over a wide temperature range ($0.7 \leqslant T \leqslant 2$), but still clearly above the temperatures T_F and T_2 (remember that $\beta_F \equiv 1/T_F \approx 1.88$, $\beta_2 \equiv 1/T_2 = 2.0$). Also included are the theoretical predictions for $N \to \infty$ obtained within the replica-symmetric and one-step replica-symmetry-breaking theory, respectively. This figure reveals unexpectedly large finite-size effects over a broad temperature regime in that, e.g., the energy for $N = 640$ coincides with the asymptotic result only if $\beta \lesssim 0.6$. For $\beta \gtrsim 0.6$ clear deviations from the asymptotic solution are visible, which are larger for smaller N. The numerical data for finite N, in the range accessible to our work, reveal only a smooth crossover from the regime of the disordered high-temperature phase to the regime of the low-temperature glass-like phase, and no indication of the kink at β_0, predicted by the one-step replica-symmetry-breaking theory, is yet visible. As expected even for $N \to \infty$, there is no effect of the dynamical transition at $\beta_D \equiv 1/T_D$ on static quantities like the energy.

Of course it is also of interest to study how at fixed temperature the energy $e_N(T)$ converges to its asymptotic limit $e_\infty(T)$. Figure 1(*b*) shows that the energy difference $e_N(T) - e_\infty(T)$ scales like N^{-1} both for temperatures above the static transition temperature T_0 and for temperatures below T_0, while at T_0 a different law, $\left(\propto N^{-2/3}\right)$, seems to hold (see the inset). (Note that we plot here data for T_D instead of T_0 since we have simulated more system sizes at this temperature. However, since the two temperatures are so close to each other this difference should not matter for the system sizes investigated here.)

We have also calculated the temperature dependence of the entropy $s(T)$. This was done by a thermodynamic integration [52] of the free energy f:

$$s(\beta) = \beta e(\beta) - \bar{\beta} f(\bar{\beta}) + \int_{\bar{\beta}}^{\beta} e(\beta)\, \mathrm{d}\beta. \tag{28}$$

We have used $\bar{\beta} = 0.5$, a temperature at which our data are no longer sensitive to finite-size effects and thus the replica solution is valid, so we can use for the free energy $\bar{\beta} f(\bar{\beta}) = \beta e(\bar{\beta}) - s(\bar{\beta})$ the mean-field value $-9/16 - \log(10)$ (see equation (25)). The integral over e was done by using a spline interpolation of our data, with 180 points for $N = 160$, 320, 640 and 100 points for $N = 1280$, 2560. We think that alternative methods for calculating $e(T)$, such as re-weighting techniques or methods of directly sampling the density of states [48], would not provide a significant advantage in our case. The results are shown in figure 1(*c*) from which we recognize that $s(T)$ shows similar finite-size effects to the energy $e(T)$.

From equation (25) we see that the entropy at the static transition is

$$s(T_0) = \ln 10 - \tfrac{9}{4}(T_s/T_0)^2 \approx 0.544 \qquad \text{i.e. } s(T_0)/s(T=\infty) \approx 0.236. \tag{29}$$

Thus we see that, while at the static transition temperature T_0 the entropy has decreased to less than a quarter of its high-temperature value, it is clearly non-zero (and non-negative, of course). In supercooled liquids one often extrapolates the temperature dependence of the entropy (minus the vibrational entropy of the crystal) to zero and uses this to define the Kauzmann temperature T_K [31]. If one proceeds in the same way with the current model to obtain a 'Kauzmann temperature' T_K where the entropy of the metastable high-temperature phase vanishes, one obtains from equation (25)

$$T_K/T_s = \tfrac{3}{2}(\ln 10)^{-1/2} \approx 0.9885 \tag{30}$$

which is even below the 'true' metastability limit $T_s = 1$ of the disordered phase, where the (extrapolated) static glass susceptibility is divergent. (Note that the proximity of T_K and T_s happens coincidentally for $p = 10$. For example, for $p = 5$ the general result [7]

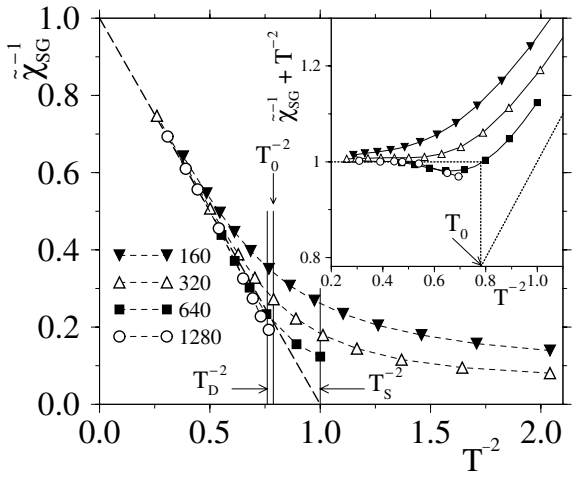

Figure 2. Inverse of the reduced spin glass susceptibility $\tilde{\chi}_{SG}$ versus the square of inverse temperature for different system sizes (curves with symbols). The solid line shows the result from the replica-symmetric theory, equation (26). Inset: a plot of $\tilde{\chi}_{SG}^{-1} + (T_s/T)^2$ to illustrate the non-monotonic convergence towards equation (26). See the main text for more details.

$T_K/T_s = \left[\frac{1}{4}(p-1)/\ln p\right]^{1/2}$ implies $T_K/T_s \approx 0.7882$.) Also a strictly linear extrapolation of $s(T)$ from T_s or T_0 down to a temperature where this extrapolation would vanish does not give a meaningful result, of course.

These results show that the idea of locating the static glass transition temperature by an extrapolation of the (configurational) entropy function $s(T)$ in the disordered high-temperature phase to $s(T = T_K) = 0$ [31, 32] can be completely misleading, even for a mean-field model that does indeed exhibit both a dynamical transition (at T_D) and a static transition (at T_0). While T_K is always lower than T_0, it does not coincide with the stability limit of the metastable high-temperature phase, and thus lacks any physical significance. Since for the case of polymers theories were formulated that suggest that T_K is the static glass transition temperature [32], it is interesting to note that a simulation study of the glass transition in the framework of the bond-fluctuation model found a decrease of s from its high-temperature value to about $1/4$ of this value, when T is lowered, but that subsequently the curve $s(T)$ versus T bends over and a well-defined T_K does not exist [54]. The 'configurational entropy' estimated by Gibbs and DiMarzio [32] was simply the total entropy of their lattice model of polymers, just like the total entropy of our model shown in figure 1(*c*). Thus this demonstrates that the T_K calculated in this way is most probably wrong. Of course, this 'naive' way to define the Kauzmann temperature via the vanishing of the (configurational) entropy $s(T)$ should not be confused with the approach of defining a 'complexity' [5, 22–27, 70]. In that approach one determines the number of basins in the *free* energy and defines T_K as that temperature at which this number starts to become exponentially large.

Note that in general one has to distinguish the 'complexity' from the configurational entropy (e.g. in a real structural glass this quantity is defined by subtracting the vibrational entropy from the total entropy of the glass), although in much of the literature on mean-field models (which lack any vibrational entropy, like the present one) the complexity is also called configurational entropy, unlike the nomenclature used here. A quantitatively reliable estimation of the complexity for the present model is rather difficult since the temperature interval of interest ($T_0 < T < T_D$) where the complexity is meaningful (basins of phase space separated by infinitely high barriers in the thermodynamic limit) is very narrow.

Figure 2 shows the reduced spin glass susceptibility as a function of the squared inverse temperature. This representation is adapted to the theoretical temperature dependence of this quantity—see equation (26)—which predicts at T^{-2}-law at high temperatures. As expected

already from the behaviour of the internal energy, even far above T_s and T_0 the convergence to the thermodynamic limit is rather slow. Unfortunately the analysis of the finite-size behaviour of $\tilde{\chi}_{SG}$ is not straightforward, as we will show in the following. For $T < T_0$ and $N \to \infty$, equations (10) and (22) imply

$$\tilde{\chi}_{SG}^{-1} = \frac{p-1}{Nq_0^2} \frac{1}{(1 - T/T_0)} \tag{31}$$

since for $T < T_0$ our definition for $\tilde{\chi}_{SG}$, equation (10), simply picks up a contribution due to the non-zero spin glass order parameter q_0. As a result, $\tilde{\chi}_{SG}^{-1}$ for $N \to \infty$ should follow the straight dashed line in figure 2 that represents the replica-symmetric solution for all $T^{-2} < T_0^{-2}$, while for $T^{-2} > T_0^{-2}$, $\tilde{\chi}_{SG}^{-1}$ simply converges towards the abscissa. This singular behaviour of $\tilde{\chi}_{SG}^{-1}$ is explained further in the inset, where we have added to $\tilde{\chi}_{SG}^{-1}$ the term $(T_s/T)^2$. This sum gives unity for $T > T_0$ and $(T_s/T)^2$ for $T < T_0$, as can be seen from equation (26). For very large but finite N, $\tilde{\chi}_{SG}^{-1}$ for $T < T_0$ exhibits a Curie–Weiss-type divergence at T_0, but the amplitude of this effect is only of order $1/N$, as can be seen from equation (31). In order to analyse the finite-size rounding of this singularity, one must consider that for N finite the δ-functions in equation (22) are broadened into peaks of finite height and non-zero width[4]. Our simulation results for $P(q)$—see figure 3—do indeed give evidence that a second peak at $q_0 \neq 0$ develops, distinct from the peak at small q that exists also in the high-temperature phase. However, the statistical accuracy of $P(q)$ is not very high due to the well-known fact that in the ordered phase this quantity is not self-averaging [22–27], and the number of realizations of the random couplings that we were able to study is insufficient to overcome this problem. Hence we are currently not able to do a proper analysis of the finite-size effects of $P(q)$—see figure 3(b)—and thus cannot make a finite-size analysis of $\tilde{\chi}_{SG}$.

From figure 3(a) we see that even in the high-temperature phase, i.e. for $T > T_0$, we see a peak in $P(q)$ at a *finite* value of q. That this is, however, a finite-size effect is demonstrated in figures 3(b) and 3(c) where we plot $P(q)$ for different system sizes and show the first moment of $P(q)$ as a function of N, respectively. We see that for temperatures well above T_0 the first moment vanishes like $N^{-1/2}$. However, close to T_0 this type of extrapolation would give a *finite* value of the moment. If instead an extrapolation with $N^{-1/3}$ is done—see the inset—one finds again as expected that the moment vanishes. Note that for the second moment of $P(q)$ we would have at $T = T_0$ again a scaling of the type $N^{-2/3}$, as we found for the case of the energy. It is interesting to note that Parisi *et al* [71], making use of a replica-symmetry-breaking scheme, were able to calculate the finite-size scaling exponents for the Ising spin glass, and obtained that $\left[\langle q^k \rangle\right]$ scales like $N^{-k/3}$ at the critical temperature (consequently one has that e scales like $N^{-2/3}$). It is thus possible that the same kind of scaling holds also for the Potts glass, although one has to keep in mind that the natures of the transition and of the replica-symmetry-breaking pattern are different.

While the results shown so far demonstrate a rather encouraging qualitative consistency between the theoretical predictions and the numerical data, our results for the fourth-order cumulant g_4, equation (11), and the Guerra parameter G, equation (12), are clearly rather worrisome (figure 4). It is seen that the three curves for $g_4(N, T)$ have a rather well-defined common intersection point at $T \approx 1.31$, and the three curves for $G(N, T)$ have a rather well-defined common intersection point at $T \approx 1.24$. On the basis of standard knowledge and experience with finite-size scaling at second-order [48,55] and first-order [48,56] phase transitions, such intersection points are commonly taken as estimates of the transition temperature [22–27]. However, the

[4] A phenomenological attempt to describe the finite-size behaviour for the glass transition of Potts models has been made in [16], but this approach is not followed up here, since it is not consistent with equation (22) in the limit of $N \to \infty$.

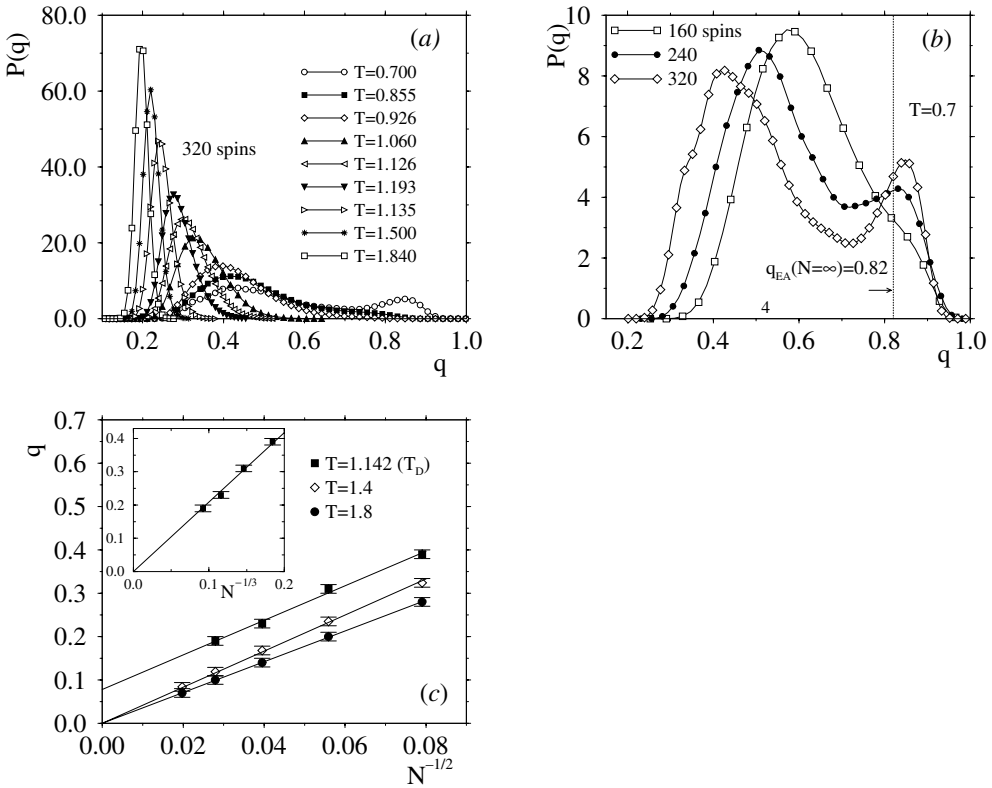

Figure 3. (*a*) Order parameter distribution $P(q)$ versus q for $N = 320$ and various temperatures. (*b*) Order parameter distribution $P(q)$ versus q for $T = 0.7$ and the three system sizes $N = 160$, 240 and 320. The asymptotic value of the order parameter (from [53]) is included as a vertical line. (*c*) Value of the first moment $\int q P(q)\, dq$ of the order parameter distribution versus $N^{-1/2}$. The inset shows that close to the transition temperature $T_0 \approx T_D$ this moment scales like $N^{-1/3}$.

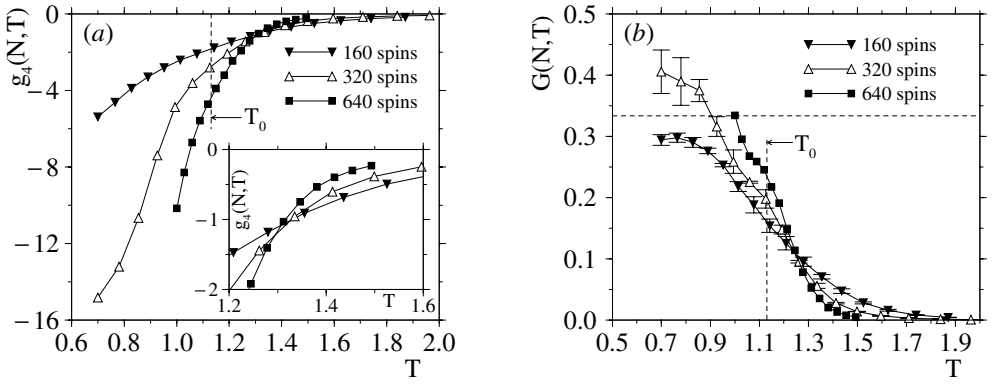

Figure 4. (*a*) Fourth-order cumulant g_4 plotted versus temperature, for three values of N, $N = 160$, 320 and 640. The vertical straight line shows the predicted static transition temperature T_0. (*b*) The same as (*a*), but for the Guerra parameter. The horizontal dashed line shows the theoretical expectation for $T < T_0$.

comparison with the exact result for T_0, equation (24), shows that these intersection points are spurious, and hence cannot be taken as accurate estimates of T_0. This is already obvious from the data alone, because the two quoted temperatures are not in mutual agreement. We think that in reality neither the three curves for $g_4(N, T)$ nor those for $G(N, T)$ intersect at a unique temperature. Given the relatively large error bars of the data, they can only define temperature intervals ΔT_{g4}, ΔT_G, in which the three intersection points fall. As $N \to \infty$, presumably all of the temperatures of these intersections converge (slowly!) towards T_0. Since T_0 falls distinctly outside the above intervals, this method of searching for intersection points, which is so successful for locating phase transitions in pure systems [48,55,56], is a complete failure here. We emphasize this problem so strongly because such techniques are commonly used for studying phase transitions in systems with quenched disorder [27]. Again we stress that analytical guidance for the description of the finite-size rounding of first-order glass transitions would be very useful.

The question of finite-size effects at a first-order transition in a disordered system has also been addressed by Stiefvater *et al* [57] in the context of the capacity problem in the Hopfield model. These authors assumed that the fractions f, $1-f$ of the two phases scale as $f/(1-f) \approx \exp\{a - Nb(\alpha - \alpha_c)\}$, where a, b are constants and α is the control parameter of the model, α_c being the transition point. However, this form implies that in the thermodynamic limit $f = 1$ for $\alpha < \alpha_c$ and $f = 0$ for $\alpha > \alpha_c$, just as for standard first-order phase transitions which have a latent heat. If this ansatz is true for the Hopfield model, it completely differs from our case where the weight of the ordered phase vanishes continuously rather than discontinuously, $f \propto (1 - T/T_0)$ as $T \to T_0$, in the thermodynamic limit (see figure 5(*b*)).

4. Dynamical properties in the high-temperature phase

In this section we briefly review the theoretical predictions for the relaxation dynamics of the spins. Subsequently we compare these predictions with the results from the simulations.

The theoretical results of Kirkpatrick *et al* show that the Potts glass with $p > 4$ states has a 'dynamical transition' at a temperature $T_D > T_0$, where non-ergodicity sets in [5]. For $T \leqslant T_D$, the spin-correlation function $C(t)$, defined in equation (13), no longer decays to zero but gets stuck for $t \to \infty$ at a non-zero value $q_{\mathrm{EA}}(T)$, with [13]

$$T_D = 1.142 \qquad q_{\mathrm{EA}}(T = T_D) = 0.328. \tag{32}$$

The details of this transition from ergodic (for $T > T_D$ where $C(t \to \infty) = 0$) to non-ergodic behaviour (for $T < T_D$), as well as the time dependence of $C(t)$ for temperatures around T_D are in fact described by equations [5] formally analogous to equations proposed for the structural glass transition by idealized mode-coupling theory [6]. The qualitative behaviour of various quantities expected for $N \to \infty$ is sketched in figure 5. Note that for $T > T_D$ and $T < T_0$ we have $q_0 = q_{\mathrm{EA}}$. In the temperature range $T_0 < T < T_D$ we have, however, $q_0 = 0$ and $q_{\mathrm{EA}} > 0$.

In figure 6(*a*) we show the time dependence for the spin-autocorrelation function $C(t)$ for $N = 1280$ and all temperatures investigated. Here and in the following we will measure time in units of Monte Carlo steps (MCS), i.e. the average number of updates per spin. Surprisingly we see that even for this rather large system size there is not yet any clear evidence for the development of a plateau for temperatures around T_D. Note that in the thermodynamic limit this function should at $T = T_D$ decay to q_{EA}, i.e. the horizontal line. In contrast to this, our system with a finite size is always ergodic, since the free-energy barriers separating the various 'valleys' in phase space remain finite at all non-zero temperatures. Of course every finite system with no hard-core interactions is in principle ergodic. However, e.g. in structural glasses it is found that even a few hundred particles are sufficient to show a pronounced (effective) ergodic-to-non-ergodic transition. Thus it is rather astonishing that for the present model the

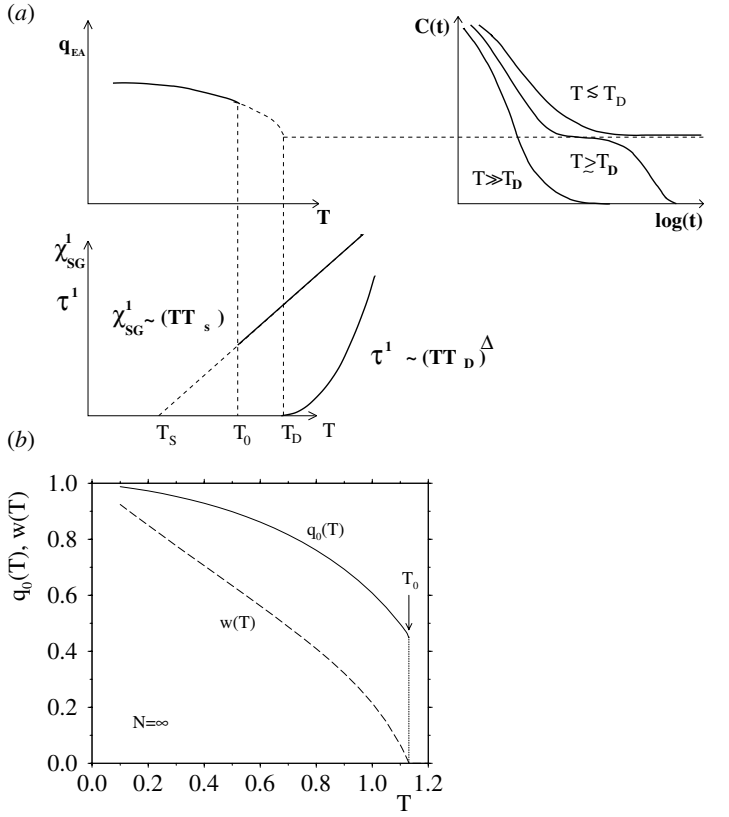

Figure 5. (*a*) A qualitative sketch of the mean-field predictions for the p-state Potts glass model with $p > 4$. The spin glass order parameter, q_{EA}, is non-zero only for $T < T_0$ and jumps to zero discontinuously at $T = T_0$. The spin glass susceptibility χ_{SG} follows a Curie–Weiss-type relation with an apparent divergence at $T_s < T_0$; see equation (21). The relaxation time τ already diverges at the dynamical transition temperature T_D. This divergence is due to the occurrence of a long-lived plateau of height q_{EA} in the time-dependent spin-autocorrelation function $C(t)$. From Brangian *et al* [58]. (*b*) The temperature dependence of q_0 and $w(T)$ (see equation (22)) for $p = 10$, as obtained from the one-step replica-symmetric solution of De Santis *et al* [13].

finite-size effects are so strong that even for $N = 1280$ and at $T = T_D$ the existence of a plateau can hardly be seen.

Also the time dependence of $C_{RI}(t)$—equation (14)—shows strong finite-size effects, as can be seen from figure 6(*b*). We see that, contrary to naive expectation, the long-time limit of $C_{RI}(t)$ is not zero but a finite constant. This constant depends on temperature and below we will discuss its origin and its dependence on system size in more detail. At any rate, we see that this correlation function also does not show a plateau even if T is close to T_D and hence we conclude that $C_{RI}(t)$ also converges only very slowly to its behaviour in the thermodynamic limit.

In order to discuss the system size dependence of the correlation functions in more detail we show in figure 7 $C(t)$ and $C_{RI}(t)$ for different system sizes and two temperatures. From figure 7(*a*) we see that, at high temperatures, $C(t)$ shows basically no system size dependence. For low T, however, the relaxation becomes quickly slower with increasing system size and also the shape of the curve changes noticeably. But even at the largest system sizes accessible at this temperature we are not able to see a clear two-step relaxation such as one would expect for a sufficiently large *but finite* system.

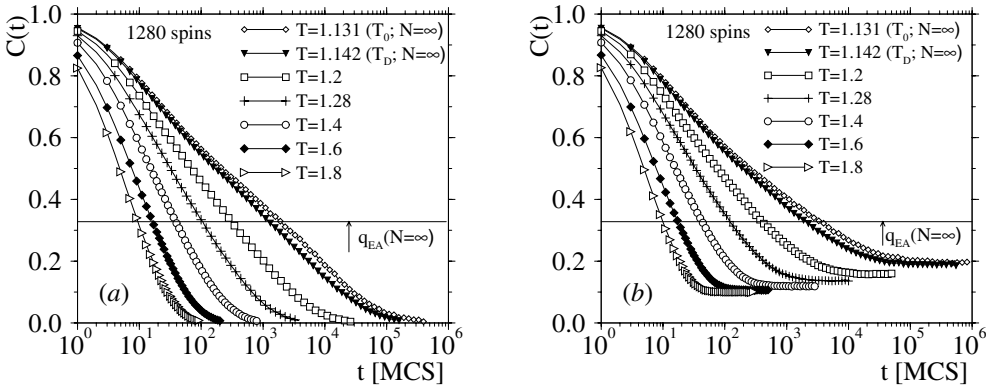

Figure 6. (*a*) The time dependence of the correlation function $C(t)$—equation (13)—for $N = 1280$ and various temperatures. Also included are data for the predicted values of the static, T_0, and dynamic, T_D, transition temperatures. The horizontal straight line shows the theoretical prediction from [13] for the Edwards–Anderson order parameter at T_D, $q_{\rm EA} = \lim_{t\to\infty} C(t)$; cf. equation (32). (*b*) The same as (*a*), but for the rotationally invariant correlation function $C_{RI}(t)$ defined in equation (14).

The N-dependence is different in the case of $C_{RI}(t)$; figure 7(*b*). Here we see that even at high temperatures the correlation function depends on the system size. This is in agreement with the arguments given in the context of equation (14) that $C_{RI}(t \to \infty)$ should scale like $1/\sqrt{N}$. That one actually find this size dependence is shown in the inset of figure 7(*b*). Instead of studying the function $C_{RI}(t)$ one could of course try to consider the reduced normalized function $\phi(t) = [C_{RI}(t) - C_{RI}(t \to \infty)]/[C_{RI}(0) - C_{RI}(t \to \infty)]$. However, this type of correlation function also has its problems since on one hand the final asymptote $C_{RI}(t \to \infty)$ is only known to within a certain statistical error, and on the other hand it shows finite-size effects at high temperatures at *short* times, i.e. where $C_{RI}(t)$ is independent of N. In view of these problems with $C_{RI}(t)$ we will in the following focus on $C(t)$ only. However, this is not a serious restriction, since in the thermodynamic limit these two functions should show at low temperatures the same time dependence anyway. That this is indeed the case for the simulations can be inferred from figure 7(*c*) where we show a parametric plot of $C_{RI}(t)$ versus $C(t)$ at T_D. We see that with increasing system size the curves do approach the diagonal, as expected.

We now address the dependence on temperature and N of the relaxation time τ of the system. One possibility for defining τ is

$$C(t = \tau) = 0.2. \tag{33}$$

Note that although the value 0.2 is somewhat arbitrary, it is a reasonable choice. The only important thing is that it is significantly less than the height of the plateau in the thermodynamic limit, $q_{\rm EA}(T = T_D)$; cf. equation (32). (If we defined a time τ' as $C(t = \tau') = 0.5$, on the other hand, τ' would be finite also below T_D, and even below T_0, until $q_{\rm EA}(T)$ had increased up to $q_{\rm EA} = 0.5$, due to the temperature dependence of the order parameter; see figure 5(*a*).)

Since for $N \to \infty$ the dynamics of the model should be described by (idealized) mode-coupling theory [5], we expect $\tau(T)$ to show a power-law divergence at T_D [6]:

$$\tau \propto (T/T_D - 1)^{-\Delta} \qquad N \to \infty \tag{34}$$

where Δ is an exponent which is non-universal (i.e. model dependent), but typically not very different from $\Delta \approx 2$. In order to test the validity of equation (34), one can plot $\tau^{-1/\Delta}$ for a

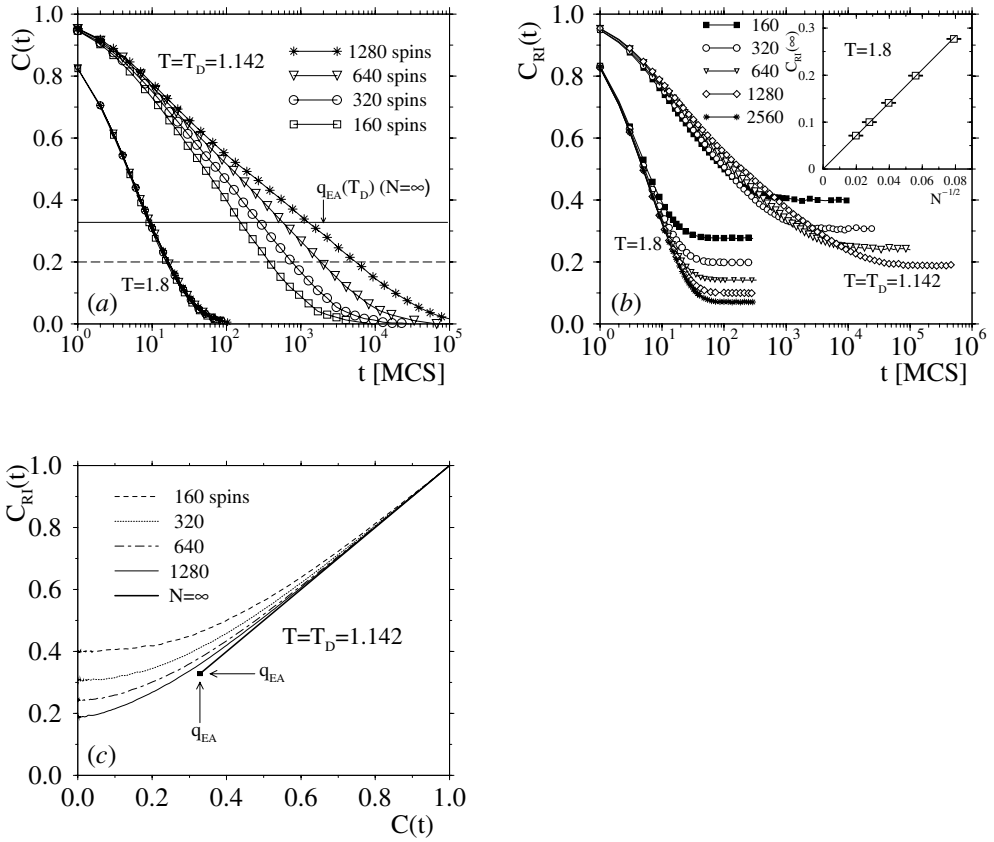

Figure 7. (*a*) The time dependence of the correlation function $C(t)$ for $T = 1.8$ and for $T = T_D = 1.142$ for several values of N. The solid line shows the theoretical value of the Edwards–Anderson order parameter $q_{\rm EA}(T_D)$ for $N \to \infty$ [13]. The dashed line shows the value that we use to define the relaxation time τ. From Brangian *et al* [58]. (*b*) The time dependence of the rotationally invariant correlation function $C_{RI}(t)$ for $T = 1.8$ and for $T = T_D = 1.142$ for several values of N. The inset shows the limiting value $C_{RI}(t \to \infty)$ as a function of $N^{-1/2}$ for $T = 1.8$. (*c*) A parametric plot of $C_{RI}(t)$ versus $C(t)$ at $T = T_D$ for different values of N. The filled square indicates the plateau value obtained for $N \to \infty$. The bold straight line displays the relation $C_{RI}(t) = C(t)$, believed to hold for $N \to \infty$.

reasonable trial value of Δ and look at whether the data are compatible with a straight line over a reasonable range of temperature. If this is the case then the extrapolation to $\tau^{-1/\Delta} = 0$ should give an estimate for T_D. Figure 8 shows that for $\Delta = 2.0$ the data are indeed rectified for $1.1 \leqslant T \leqslant 1.4$, while outside of this temperature range the curves bend. Since plots for other reasonable choices of Δ look quite similar, the value of Δ can be estimated only within ± 0.5. In all cases it is difficult to use the estimates for T_D for finite N to extrapolate to the value of T_D in the thermodynamic limit, since the N-dependence is rather weak and the error bars of $T_D(N)$ are, due to the above-mentioned extrapolation, quite substantial. For the case of $\Delta = 2.0$ a dependence of the form $T_D(N) - T_D(\infty) \propto 1/N$ seems, however, to be compatible with the data [51].

In order to provide a more systematic way of extrapolating the relaxation times to the thermodynamic limit, we assume that the dynamical finite-size scaling hypothesis [55, 59, 60] holds and make the ansatz

$$\tau = N^{z^*} \tilde{\tau} \left\{ N(T/T_D - 1)^{\Delta/z^*} \right\} \qquad \text{for } N \to \infty \text{ and } (T/T_D - 1) \to 0. \tag{35}$$

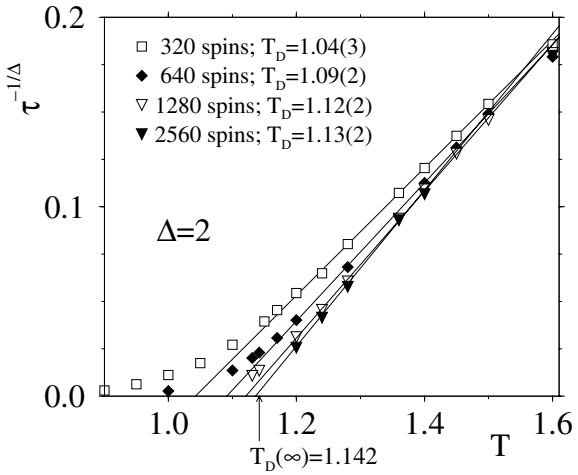

Figure 8. The temperature dependence of $\tau^{-1/\Delta}$ for different system sizes, using $\Delta = 2.0$ as a trial value. The bold straight lines are fits to a proper subset of points. The resulting extrapolated values for $T_D(N)$ are quoted in the figure.

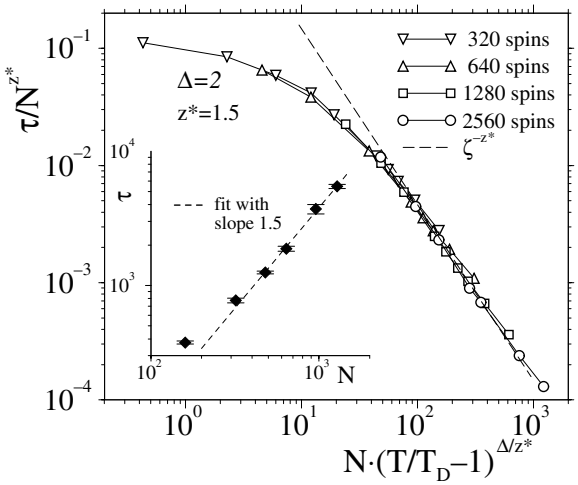

Figure 9. A log–log plot of the scaled relaxation time τ/N^{z^*} versus the scaled distance $N(T/T_D - 1)^{\Delta/z^*}$ from the dynamical transition temperature T_D, choosing $z^* = 1.5$ and $\Delta/z^* = 1.3$. The inset is a log–log plot of $\tau(T = T_D)$ versus N.

The scaling function $\tilde{\tau}(\zeta)$ must obey $\tilde{\tau}(\zeta \to \infty) \propto \zeta^{-z^*}$ to recover the proper thermodynamic limit, i.e. equation (34). Using z^* as a fit parameter (Δ is fixed to 2.0), we thus can try to generate a master curve from the $\tau(T)$ curves for the different system sizes N. That this is indeed possible if one chooses $z^* = 1.5$ is shown in figure 9. From this figure we see that for large arguments the master curve does indeed show the expected power law with an exponent $-z^*$ (dashed line). For $T = T_D$ the argument of $\tilde{\tau}$ vanishes and hence we expect an N-dependence of τ of the form $\tau \propto N^{z^*}$, and the inset of figure 9 shows that this is indeed the case.

We mention that equation (35) has a firm theoretical foundation for second-order phase transitions [22, 55, 59, 60], i.e. the case in which in figure 5 the temperatures T_0, T_D and T_s coincide at a unique critical temperature T_c. The diverging relaxation time is then an immediate consequence of a diverging static susceptibility, and dynamic finite-size scaling is a consequence of ordinary dynamic scaling [60]. For example, for second-order transitions of mean-field spin glass models one has equation (35) with $\Delta/z^* = \gamma_{MF} + 2\beta_{MF} = 3$, since the static mean-field exponents of the spin glass order parameter and susceptibility are $\beta_{MF} = 1$ and $\gamma_{MF} = 1$, respectively [22]. Using the value of $\Delta = 2$ [22], one hence finds for z^* the value $2/3$. This result could be expected since the standard finite-size scaling result for the

critical relaxation in spin glasses *with short-range interactions* is $\tau \propto L^z$ with $z = 4$ in the mean-field approximation [22]. (Here L is the linear dimension of the system.) This result can now be translated into the behaviour of infinite-range models at the marginal dimension $d^* = 6$, i.e. at the dimension where mean-field theory becomes valid, via $N = L^{d^*}$, which yields $\tau \propto N^{z/d*} = N^{z^*}$, i.e. $z^* = z/d^* = 2/3$. This result is also compatible with numerical simulations [61]. However, the value $z^* \approx 1.5$ found for the present model is clearly rather unusual and we are not aware of any analytical estimates for this exponent.

A further interesting question concerns the asymptotic decay of the correlation function $C(t)$ towards q_{EA} as $t \to \infty$ at $T = T_D$. In the context of the structural glass transition, the time regime during which the correlation functions are close to the plateau is called the 'β-relaxation' whereas the decay below the plateau is called the 'α-relaxation' [6]. Mode-coupling theory predicts that at T_D the approach to the plateau is given by a power law, i.e.

$$C(t) - q_{\mathrm{EA}} \propto t^{-a} \qquad T = T_D. \tag{36}$$

Unfortunately, due to the lack of clear evidence for a plateau in our data, we cannot present a fully convincing test of this prediction although we have evidence that our data are indeed compatible with the dependence given in equation (36) [51].

Two other important results from mode-coupling theory concern the shape of the correlators close to T_D in the α-relaxation regime, i.e. in the time window where they fall under the plateau. The theory predicts that in this time regime the correlators can be approximated well with the Kohlrausch–Williams–Watts function, $\exp(-(t/\tau)^{\beta})$, a functional form that has been found to work very well in many glassy systems [6, 33, 35, 39]. We find, however, that even close to T_D and for the largest systems used, this functional form does not give a good fit to the data.

The second prediction of the theory concerning the α-relaxation is the so-called time–temperature superposition principle. This principle implies that the correlator $C(t)$ can be written as

$$C(t, T) = \tilde{C}(t/\tau(T)) \tag{37}$$

where $\tilde{C}(x)$ is a temperature-independent scaling function. The validity of equation (37) can be checked if one plots $C(t, T)$ versus $x = t/\tau(T)$. If the superposition principle is valid, the curves for the different temperature should fall on a master curve for $x \approx 1$ and large x. For very small values of x, i.e. in the early β-regime, no master curve is expected, since equation (37) is supposed to hold only in the α-regime. Figure 10 shows this kind of scaling plot and we see that even for a rather large system, $N = 1280$, there is no indication of such a time–temperature position principle. Of course, it is possible that this failure to bear out equation (37) is simply due to finite-size effects. Thus, it would be desirable to check equation (37) for much larger systems. However, in view of the strong size effects on the relaxation time τ near and below T_D—see figure 12 below—this is impossible for us with the present computer resources.

Although we have just seen that the time–temperature superposition principle does not hold close to T_D *for the accessible system sizes*, it is interesting to see whether this is the case also at lower temperatures. For $N = 160$ we have been able to go to temperatures as low as $T = 0.7$, and in figure 11 we show the correlator as a function of t/τ. If the curves for all temperatures are considered, one finds that the superposition principle again does not hold (main figure). However, if one uses only the curves for the lowest temperatures—see the inset—one finds that they all collapse onto a nice master curve. Thus we conclude that at sufficiently low temperatures the time–temperature superposition principle does indeed hold. We mention also that the shape of this master curve is *not* an exponential, but that a stretched exponential with an exponent around 0.43 gives a satisfactory fit.

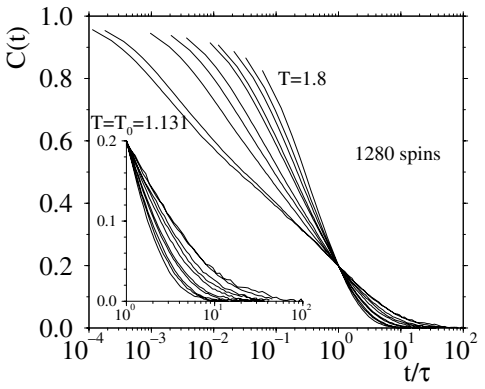

Figure 10. A plot of $C(t)$ versus t/τ (where τ is defined via $C(t = \tau) = 0.2$; cf. equation (33)), for $N = 1280$. Temperatures from right to left: $T = 1.8$, 1.6, 1.5, 1.4, 1.360, 1.280, 1.240, 1.2, 1.142 and 1.131. The inset shows a magnification of the part of the curves for $t/\tau > 1$.

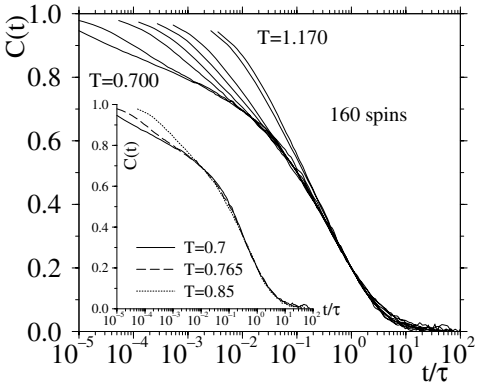

Figure 11. A plot of $C(t)$ versus t/τ for $N = 160$. The temperatures are $T = 0.7$, 0.765, 0.85, 0.9, 0.95, 1.0, 1.142 and 1.17 (left to right). The inset shows the same data, but including only the three lowest temperatures.

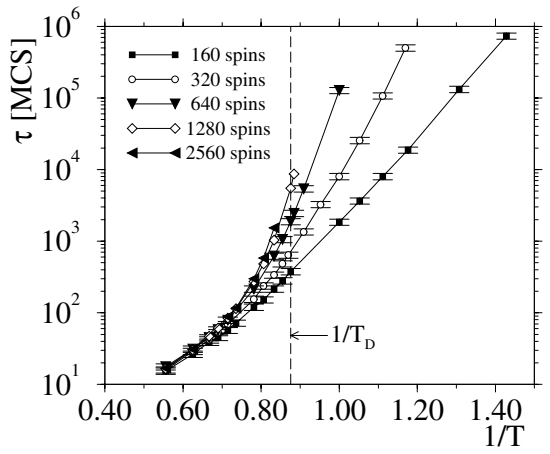

Figure 12. Relaxation time τ plotted versus inverse temperature for different system sizes. The broken vertical line indicates the location of the dynamical transition. Note the choice of a logarithmic scale for the ordinate. The error bars of τ are mostly due to the sample-to-sample fluctuation.

In order to be able to understand this result a bit better, one needs to understand in more detail the relaxation of our model for $T < T_D$ and finite N, where all free-energy barriers in phase space must obviously be still finite. One could argue that at low temperature the largest barrier dominates the dynamics and hence the relaxation depends on temperature only via a temperature-dependent prefactor. This temperature dependence would have to be Arrhenius-like, and in order to check this we show in figure 12 the T-dependence of τ for the different system sizes.

From this figure we see that at the lowest temperatures the T-dependence of τ for the smallest system is indeed Arrhenius-like. For temperatures around T_D and higher, one sees however significant deviation from this type of temperature dependence. Also for $N = 320$ one can see at the lowest temperature an Arrhenius law, but the activation energy is significantly larger than the one for $N = 160$. Since for increasing system size the lowest accessible temperature becomes higher and higher, it is not possible to see any longer the crossover from the non-Arrhenius T-dependence at intermediate temperatures to the Arrhenius dependence

at small T. But the plot clearly shows that at T_D the relaxation times increase quickly with increasing system size, in agreement with the result from figure 9 (inset). Due to our present inability to equilibrate larger systems also significantly below T_D, we cannot determine reliably the N-dependence of the activation energy of the Arrhenius law found at low temperatures. We mention that MacKenzie and Young found for the SK model, i.e. the mean-field Potts glass for $p = 2$, that for small systems ($N \leqslant 128$) and low temperature ($T = 0.6T_D = 0.6T_s$) the relaxation times increase like $\tau(N) \propto \exp(\text{const} \times N^{0.5})$ [63] whereas in a recent paper Billoire and Marinari [64] give evidence that the exponent of the power law is $1/3$. If we consider a low temperature, $T = 0.7$, this type of N-dependence of τ is compatible with our data with an exponent 0.5. However, if we determine the N-dependence of the activation energy in the temperature regime where $\tau(T, N)$ shows an Arrhenius law, we find that this energy increases only very slowly, i.e. like $\log(N)$ or a power of N with a small exponent ($\approx 0.1 = 1/p$). (Note that the reason for the two different N-dependencies is related to the fact that the prefactor of the Arrhenius law depends on N also.)

Figure 12 shows clearly that for small systems, $N = 160$, 320 and 640, it is possible to explore the region of temperatures below both the dynamical and the static transition. Note that in simulations of models for the structural glass transition [39] it has never been possible to explore such low temperatures for comparable numbers of particles[5]. On the other hand, such models [39] do not seem to be much plagued by finite-size effects, although for certain models for structural glasses they have recently been found [69].

5. Relaxation of individual spins in the low-temperature phase

In the previous section we have investigated the relaxation dynamics of the *whole* system and found that at low temperatures it shows a non-Debye behaviour. In the present section we focus on the dynamics of the individual spins in order to obtain a better understanding of the occurrence of this non-exponentiality.

In recent years it has been recognized that the non-exponential relaxation in supercooled liquids is often related to the so-called 'dynamical heterogeneities' [45, 46]. This means that the details of the relaxation dynamics of the individual particles (relaxation time, amplitude of the α-relaxation etc) is different for each different particle. The reason for this difference is (most likely) the fact that each particle has a slightly different neighbourhood which thus affects the dynamics of the particle. Note that these differences are present only on the timescale of the α-relaxation τ, since afterwards the particle has changed its neighbourhood and hence its characteristic dynamics. If the dynamics is averaged over a time much larger than τ, all the particles behave in the same way. For spin glasses this is different, since the disorder is quenched. Hence the nature of the dynamics of the individual spins is an intrinsic property of each spin, since each spin is connected to the other ones by a set of different coupling constants. For a spin glass with short-range interactions it is therefore not surprising that each individual spin has a different relaxation dynamics, and this is indeed what has been found in simulations [66]. For spins systems with long-range interactions the presence of such dynamical heterogeneities is, however, not that clear, since each spin interacts with many different ones and hence one might argue that on average the different spins show the same relaxation dynamics. The goal of this section is to investigate this point in more detail.

[5] An exception is furnished by simulations of strong glass formers. For example, in [65] it was shown that the system could be equilibrated even at temperatures as low as $0.8T_D$. However, this was still way above the Kauzmann temperature.

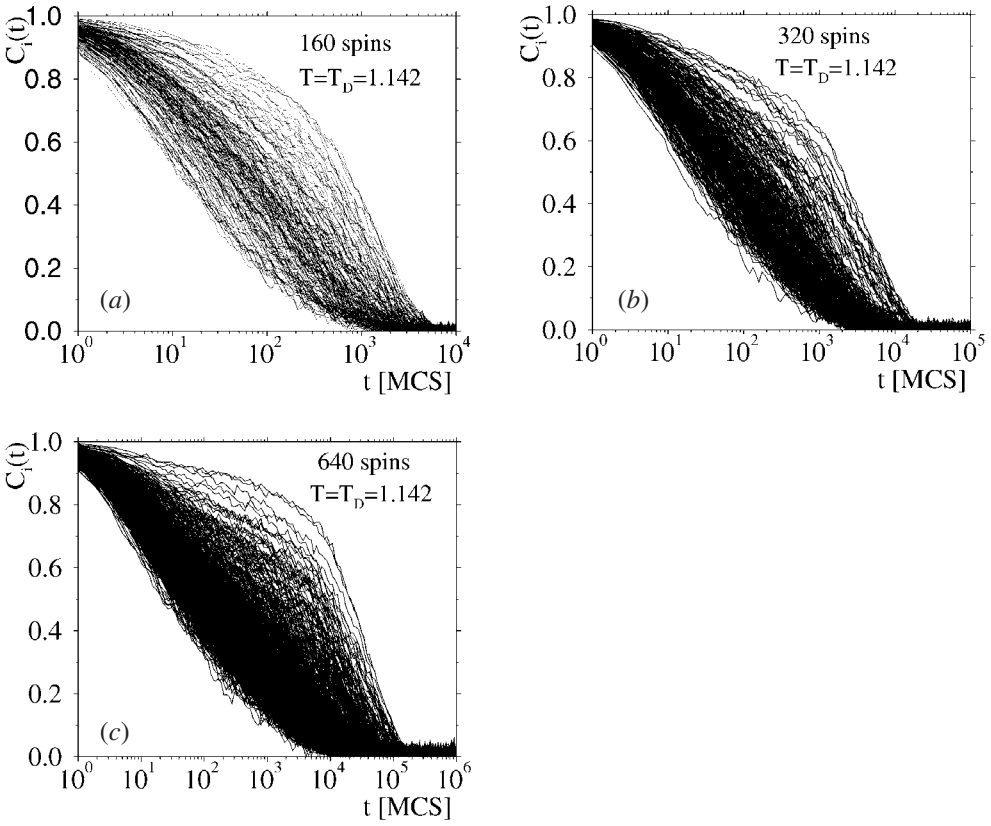

Figure 13. The time dependence of the single-spin-autocorrelation function $C_i(t)$ at $T = T_D$ for $N = 160$ (*a*), $N = 320$ (*b*) and $N = 640$ (*c*). Each of the curves corresponds to a different spin.

In order to characterize the dynamics of the individual spins we have calculated the autocorrelation functions $C_i(t)$ for spin number i:

$$C_i(t) = \frac{1}{p-1}\langle \vec{S}_i(t') \cdot \vec{S}_i(t'+t)\rangle. \tag{38}$$

Note that, in contrast to the case for structural glasses, it is here possible to average the right-hand side over different time origins t', without losing the information on the identity of the spin. Due to the single-spin nature of the correlation function $C_i(t)$, it is necessary to make this average over a sufficiently long time in order to obtain a reasonable statistics. We found that an average over 1000 α-relaxation times is needed, and therefore the following results have been obtained only for relatively small system sizes and 10 different samples for every temperature investigated.

In figure 13 we show the time dependence of $C_i(t)$ for all the spins $i = 1, \ldots, N$ for three different system sizes N. The temperature is T_D, i.e. the dynamical critical temperature at which the *average* relaxation dynamics, as measured by $C(t)$, is already strongly non-exponential. From the figure we see that the relaxation dynamics for the different spins depends strongly on these spins in that, e.g., they relax to zero on timescales that span more than an order of magnitude. At a time where the correlation functions have reached 0.5 of their initial value, the width of the range is even higher and increases rapidly with increasing system size. Furthermore, we see from the figures that the curves for the individual spins seem to occur in

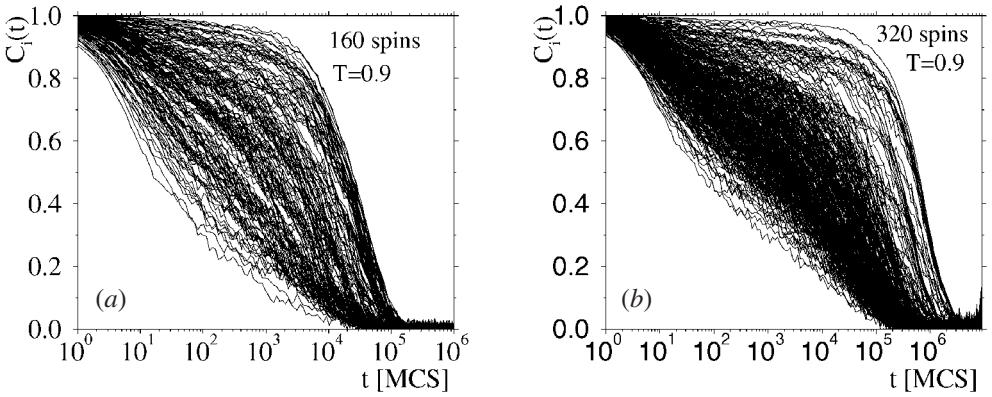

Figure 14. The time dependence of the single-spin-autocorrelation function $C_i(t)$ at $T = 0.9$ for $N = 160$ (a) and for $N = 320$ (b). Each of the curves corresponds to a different spin.

clusters, i.e. that they do not fill the interval between the slowest and the fastest relaxation in a homogeneous way. Below we will discuss the reason for this clustering in more detail.

In figure 14 we show the single-spin-autocorrelation function at a lower temperature. Comparing these curves with the ones in figures 13(a) and 13(b) we see that a decrease of T has made the distribution of the relaxation dynamics even wider. Also the presence of the clustering of the curves is now much more pronounced. From figure 14 one also recognizes that the shape of the individual curves is not uniform at all, since the ones which decay slowly tend to be, in the α-regime, much steeper than the ones that decay more rapidly. A more careful analysis shows that these slow spins show a more or less exponential relaxation whereas, as can already be seen from the figure, the fast ones show a strong deviation from a Debye law. Thus we conclude that the non-Debye behaviour of $C(t)$ found at low T—see figure 11—is not due to a superposition of Debye laws with different relaxation times, but the sum of various different processes, some of which are Debye-like, some of which are not.

In order to understand the microscopic reason for the presence of these dynamical heterogeneities a bit better we have investigated to what extent the relaxation dynamics of an individual spin correlates with other quantities. For this it is necessary to characterize this dynamics in some way. As discussed above, the shape of the curves is not at all uniform, which makes such a characterization rather difficult. Therefore we decided to neglect all the variations of the shape completely and to characterize each curve just by the time that it takes the spin to decay to a given value. Therefore we defined two different relaxation times, $\tau_i^{(0.4)}$ and $\tau_i^{(0.7)}$, via

$$C_i(t = \tau_i^{(0.4)}) = 0.4 \qquad \text{and} \qquad C_i(t = \tau_i^{(0.7)}) = 0.7. \tag{39}$$

In figure 15 we show a scatter plot between $\langle e_i \rangle$, the average energy of spin i, and the relaxation time, for both definitions of τ_i. We see that there is indeed a significant correlation between the energy and the relaxation time in that spins with high energy relax faster than the ones with low energy. This result is very reasonable since a spin that has a low energy will be reluctant to change its value and therefore to go (with high probability) to a state with a higher energy. From the figure we also recognize that the correlation is present for both definitions of τ_i, from which we conclude that the details of this definition are not crucial.

In order to investigate this point a bit more closely we show in figure 16(a) a scatter plot of the relaxation time $\tau_i^{(0.7)}$ versus $\tau_i^{(0.4)}$ for the two temperatures. We see that although the correlation is not perfect, it is still very significant and therefore we conclude that the salient

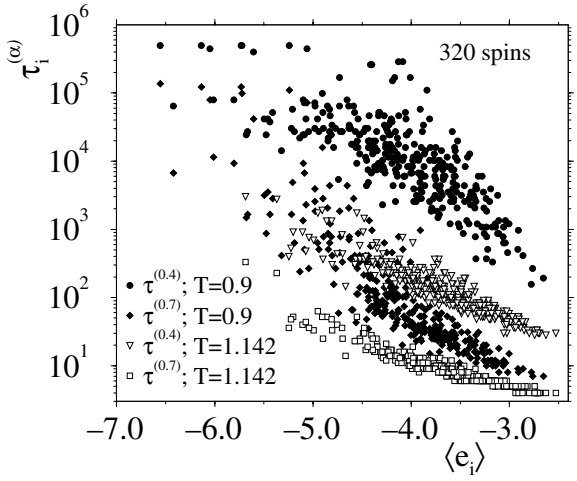

Figure 15. A scatter plot of τ_i, the mean relaxation time of spin i as defined in equation (39), versus the mean energy $\langle e_i \rangle$. The open and closed symbols correspond to $T = 1.142$ and 0.9, respectively. The points are for a typical sample of 320 spins.

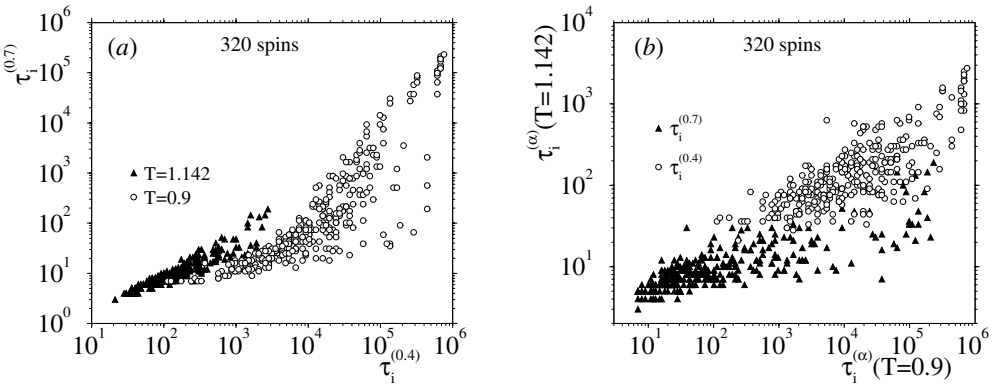

Figure 16. (*a*) A plot of $\tau_i^{(0.7)}$ (defined by $C_i(t = \tau_i) = 0.7$) versus $\tau_i^{(0.4)}$ (defined by $C_i(t = \tau_i) = 0.4$), for $T = 0.9$ and 1.142 (open and filled symbols, respectively) showing that the two relaxation times are correlated. Each point corresponds to a different spin. (*b*) A plot of the relaxation times $\tau_i^{(0.4)}$ and $\tau_i^{(0.7)}$ at $T = 1.142$ versus these relaxation times at $T = 0.9$. Each point corresponds to a different spin.

features of the correlation between the relaxation time and the mean energy shown in figure 15 will be observed even if a more careful characterization of the relaxation dynamics is made.

Of further interest is the question of how the relaxation time of a given spin at a given temperature is related to the relaxation time of the same spin at a different temperature. This dependence is related to the question of 'chaos in temperature', i.e. how the properties of a system change if temperature is changed. For a mean-field-type system these dependencies are expected to be rather weak [67, 68]. In agreement with this expectation, we find that the relaxation times τ_i for $T = 0.9$ are indeed strongly correlated with those at $T = 1.142$—see figure 16(*b*)—irrespective of the definition of τ_i. Thus we see that this property seems not to be strongly affected by finite-size effects. In passing, we also mention that the mean energies $\langle e_i(T) \rangle$ between the two temperatures are even more strongly correlated than the relaxation times [51].

Before we end, we come back to the observation discussed above that some of the single-spin-autocorrelation functions occur in clusters (see figure 14). One potential reason for the

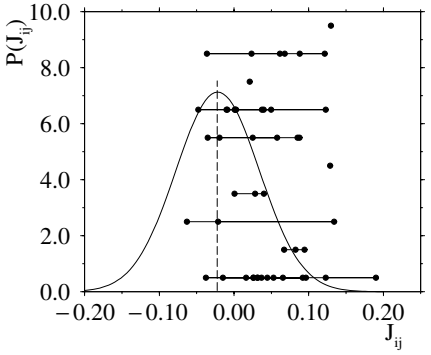

Figure 17. Values of the bonds between spins with very slow relaxation in ten different disorder realizations for 320 spins at a temperature $T = 0.9$ (filled circles). For clarity the points have been displaced vertically by various amounts. The continuous curve shows the Gaussian distribution from which the J_{ij} are extracted and the vertical dashed line shows its mean.

relaxation dynamics of two spins to be similar is that they are coupled together strongly, i.e. that their interaction constant J_{ij} is large. In order to test this idea we identified for each realization of the disorder those spins that formed at $T = 0.9$ the cluster that relaxed most slowly. (This identification was done visually by means of plots like the one shown in figure 14(b).) Say that this cluster involved k curves. We then determined the $k(k-1)/2$ interaction constants between these k spins. The values of these constants are shown in figure 17 for ten different realizations of the disorder (filled circles). Also included in the figure is the Gaussian distribution of the coupling constants given by equation (2). From this figure we see that most of the points corresponding to the couplings J_{ij} are to the right of the mean of the distribution (vertical dashed line). Hence we conclude that the spins that form the slow cluster of relaxation curves are coupled together more strongly than two arbitrary spins and therefore form a 'dynamic entity'. We note, however, that the fact that two spins are strongly coupled does not necessarily make them slow [51], which shows that such a strong coupling is only a necessary but not a sufficient condition for a slow dynamics.

It is clear that the observations presented in this section are only modest first steps addressing the dynamics of the individual spins in the low-temperature phase. It certainly would be interesting and useful to understand better how the distribution of the relaxation times of the spins depends on the system size and on temperature in order to obtain a better comprehension of how the mean relaxation dynamics of the system is related to that of the single spins. However, due to the high computational demand of this kind of investigation, such studies have to be left to the future.

In this context, we draw attention to recent interesting analysis of dynamic heterogeneities in short-ranged Ising spin glasses [72] and in a spin model based on random graphs [73]. While these models are better understood, they are probably less connected to the structural glass problem than the present one. Furthermore, we mention that recently Franz *et al* [74, 75] have proposed a connection between a certain dynamical susceptibility and the dynamical heterogeneities. Preliminary investigations have shown that this connection might work for the present model as well [51] and we will report on this in more detail elsewhere [76].

6. Conclusions

In this paper, we have presented the first detailed Monte Carlo investigation of the ten-state mean-field Potts glass model, for finite systems with sizes in the range from $N = 160$ to 2560 spins. In the thermodynamic limit, it is known that this model exhibits both a dynamical transition at T_D, where the system stops being ergodic, and a static transition at $T_0 < T_D$, where a glass order parameter q appears discontinuously (figure 5(a)). The static spin glass susceptibility χ_{SG} remains finite both at T_0 and T_D. It would diverge only

at a still lower 'spinodal' temperature $T_s < T_0$, if one were able to follow the disordered branch of the free energy at temperatures less than T_0. A further relevant temperature is the 'Kauzmann' temperature T_K—figure 1(*c*)—defined from the condition that the entropy of the high-temperature phase vanishes. The spin-autocorrelation function $C(t)$ decays with time t at $T \gtrsim T_D$ in a two-step process, and the lifetime τ of the 'plateau' diverges as $\tau \propto (T - T_D)^{-\Delta}$, in the thermodynamic limit $N \to \infty$ (figure 5(*a*)). This behaviour includes all qualitative features that one expects to be present at the structural glass transition (note that the equation of motion for $C(t)$ are identical to the ones proposed by the popular idealized mode-coupling theory for the structural glass transition!)

The questions asked in the present paper hence are as follows. Can we verify these predictions from Monte Carlo simulations? How are the various transitions modified (i.e., rounded off) by the finite size of the model systems considered? Answers to these questions are not only of interest for a better understanding of the statistical mechanics of the present model system, but also may be useful to help with the interpretation of simulations of models for the structural glass transition. First of all, in the latter case the very existence of the various temperatures T_D, T_0, T_s, T_K is still open to doubt. Secondly, even if one believes that these temperatures should exist, their location for a particular model is still uncertain, unlike in the present case where we have so much guidance from the exact solution. Of course, it is clear that a mean-field model is a rather special limit, and the sharpness of the dynamical transition at T_D is probably replaced by a smooth crossover from rather fast relaxation to very slow relaxation as soon as one allows the interactions to become short ranged. In this sense, the finite mean-field Potts glass (where the singularity at T_D is rounded by the finite size of the system) may be qualitatively similar to the finite-range model (although one should not push this analogy too far).

Gratifyingly, we have established that the Monte Carlo results are qualitatively compatible with the theoretical predictions, although the finite-size effects found were unexpectedly strong (i.e. they occur over a very wide temperature range as well) and they are not understood in detail, and hence we have found it too difficult to extract the various temperatures mentioned above directly from the simulation itself. For example, for the sizes available, the methods of looking for intersection points of the fourth-order cumulant or the Guerra parameter do not allow a reliable estimation of T_0 (figure 4). Similarly, one can estimate the temperatures T_s (figure 2), T_K (figure 1(*b*)) and T_D (figure 8) from a naive analysis of the data only very roughly. However, if one uses the theoretical knowledge on T_D, one can estimate both the exponent Δ mentioned above and the exponent z^* for the size dependence of the time τ at T_D (namely $\tau \propto N^{z^*}$) from a dynamical finite-size scaling analysis (figure 9).

We also analysed the modified disconnected cumulants proposed in [77], which should give a better estimation of the spin glass transition temperature in systems exhibiting one-step replica-symmetry-breaking patterns, but with the system sizes at our disposal they do not seem to work better than the corresponding connected parameters [51].

Regarding the shape of the curves in the α-relaxation regime, we found that the expected time–temperature superposition principle is not observed (figure 10).

Also some steps were taken to analyse the dynamics for $T \leqslant T_D$, by investigating the relaxation function $C_i(t)$ of individual spins and corresponding relaxation times (figures 13–16). We find that the reason for the observed non-exponential relaxation of the *mean* relaxation function $C(t)$ is related to the presence of a very strong dynamical heterogeneity. Furthermore, we found that certain spins form dynamical clusters, probably because of the strong bonds between them. However, this mechanism seems not to be the only one, and hence this point must be investigated in the future in more detail.

Thus, although many exact results are known for this model, and—unlike in models of the structural glass transition—we can equilibrate the system also at temperatures significantly

below T_D for a range of sizes ($N \leqslant 640$), we are still not able to answer many questions. Nevertheless, we think that the present model is a prototype model for glass transitions, and if better simulation algorithms become available, further studies of the present model should be very rewarding.

Acknowledgments

One of us (CB) was partially supported by the Deutsche Forschungsgemeinschaft, Sonderforschungsbereich 262/D1. We thank F Ritort for information on the energy versus temperature curve (figure 1(*a*)). We are grateful to the John von Neumann Institute for Computing (NIC Jülich) for a generous grant of computer time at the CRAY T3E.

References

[1] Monasson R 1995 *Phys. Rev. Lett.* **75** 2847
[2] Bouchaud J-P, Cugliandolo L, Kurchan J and Mézard M 1998 *Spin Glasses and Random Fields* ed A P Young (Singapore: World Scientific)
[3] Franz S and Parisi G 1998 *Physica* A **261** 317
[4] Mézard M and Parisi G 1999 *Phys. Rev. Lett.* **82** 747
[5] Kirkpatrick T R and Wolynes P G 1987 *Phys. Rev.* B **36** 8552
Kirkpatrick T R and Thirumalai D 1988 *Phys. Rev.* B **37** 5342
Thirumalai D and Kirkpatrick T R 1988 *Phys. Rev.* B **38** 4881
[6] Götze W 1990 *Liquids, Freezing and the Glass Transition* ed J-P Hansen, D Levesque and J Zinn-Justin (Amsterdam: North-Holland) p 287
Götze W 1990 *J. Phys.: Condens. Matter* **11** A1
[7] Elderfield D and Sherrington D 1983 *J. Phys. C: Solid State Phys.* **16** L491
Elderfield D and Sherrington D 1983 *J. Phys. C: Solid State Phys.* **16** L971
Elderfield D and Sherrington D 1983 *J. Phys. C: Solid State Phys.* **16** L1169
[8] Erzan A and Lage E J S 1983 *J. Phys. C: Solid State Phys.* **16** L55
[9] Gross D J, Kanter I and Sompolinsky H 1985 *Phys. Rev. Lett.* **55** 304
[10] Carmesin H O and Binder K 1988 *J. Phys. A: Math. Gen.* **21** 4053
[11] Cwilich G and Kirkpatrick T R 1989 *J. Phys. A: Math. Gen.* **22** 4971
Cwilich G 1990 *J. Phys. A: Math. Gen.* A **23** 5029
[12] Scheucher M, Reger J D, Binder K and Young A P 1990 *Phys. Rev.* B **42** 6881
Scheucher M, Reger J D, Binder K and Young A P 1990 *Europhys. Lett.* **14** 119
Scheucher M and Reger J D 1993 *Z. Phys.* B **91** 383
[13] De Santis E, Parisi G and Ritort F 1995 *J. Phys. A: Math. Gen.* **28** 3025
[14] Schreider G and Reger J D 1995 *J. Phys. A: Math. Gen.* **28** 317
[15] Reuhl M, Nielaba P and Binder K 1999 *Eur. Phys. J.* B **2** 225
[16] Dillmann O, Janke W and Binder K 1998 *J. Stat. Phys.* **92** 57
[17] Lobe B, Janke W and Binder K 1999 *Eur. Phys. J.* B **7** 289
[18] Marinari E, Mossa S and Parisi G 1999 *Phys. Rev.* B **59** 8401
[19] Hukushima K and Kawamura H 2000 *Phys. Rev.* E **62** 3362
[20] Edwards S F and Anderson P W 1975 *J. Phys. F: Met. Phys.* **5** 965
[21] Sherrington D and Kirkpatrick S 1975 *Phys. Rev. Lett.* **35** 1972
[22] Binder K and Young A P 1986 *Rev. Mod. Phys.* **58** 801
[23] Mézard M, Parisi G and Virasoro M A 1987 *Spin Glass Theory and Beyond* (Singapore: World Scientific)
[24] Fischer K H and Hertz J A 1991 *Spin Glasses* (Singapore: World Scientific)
[25] Stein D S 1992 *Spin Glasses and Biology* (Singapore: World Scientific)
[26] Parisi G 1992 *Field Theory, Disorder and Simulations* (Singapore: World Scientific)
[27] Young A P (ed) 1998 *Spin Glasses and Random Fields* (Singapore: World Scientific)
[28] Potts R B 1952 *Proc. Camb. Phil. Soc.* **48** 106
[29] Wu F Y 1982 *Rev. Mod. Phys.* **54** 235
Wu F Y 1982 *Rev. Mod. Phys.* **55** 315
[30] Zia R K P and Wallace D J 1975 *J. Phys. A: Math. Gen.* **8** 1495

[31] Kauzmann W 1948 *Chem. Rev.* **43** 219
[32] Gibbs J H and DiMarzio E A 1958 *J. Chem. Phys.* **28** 373
[33] Jäckle J 1986 *Rep. Prog. Phys.* **49** 171
[34] Parisi G 1987 *Complex Behavior of Glassy Systems* ed M Rubi and C Perez-Vicente (Berlin: Springer) p 111
[35] Binder K, Baschnagel J, Kob W and Paul W 1999 *Phys. World* **12** 54
[36] Coluzzi B, Verrocchio P, Mézard M and Parisi G 1999 *J. Chem. Phys.* **111** 9039
[37] Sciortino F, Kob W and Tartaglia P 1999 *Phys. Rev. Lett.* **83** 3214
[38] Crisanti A and Ritort F 2000 *Europhys. Lett.* **51** 147
[39] Kob W 1999 *J. Phys.: Condens. Matter* **11** R85
[40] Mézard M 1999 *Physica* A **265** 359
[41] Parisi G 2000 *Physica* A **280** 115
[42] Höchli U T, Knorr K and Loidl A 1990 *Adv. Phys.* **39** 405
[43] Binder K and Reger J D 1992 *Adv. Phys.* **41** 547
[44] Binder K 1998 *Spin Glasses and Random Fields* ed A P Young (Singapore: World Scientific) p 99
[45] Sillescu H 1999 *J. Non-Cryst. Solids* **243** 81
[46] Ediger M D 2000 *Annu. Rev. Phys. Chem.* **51** 99
[47] Guerra F 1996 *Int. J. Mod. Phys.* B **10** 1675
Marinari E *et al* 1998 *Phys. Rev. Lett.* **81** 1698
[48] Binder K 1997 *Rep. Prog. Phys.* **60** 487
Landau D P and Binder K 2000 *A Guide to Monte Carlo Simulations in Statistical Physics* (Cambridge: Cambridge University Press)
[49] Hukushima K and Nemoto K 1996 *J. Phys. Soc. Japan* **64** 1604
[50] Kob W, Brangian C, Stühn T and Yamamoto R 2000 *Computer Simulation Studies in Condensed Matter Physics* vol 13, ed D P Landau, S P Lewis and H B Schüttler (Berlin: Springer) p 134
[51] Brangian C 2002 *Dissertation* Johannes-Gutenberg-Universität, Mainz, in preparation
[52] Binder K 1981 *Z. Phys.* B **45** 61
[53] Ritort F Private communication
[54] Wolfgardt M, Baschnagel J, Paul W and Binder K 1996 *Phys. Rev.* E **54** 1535
[55] Binder K 1992 *Computational Methods in Field Theory* ed H Gausterer and C B Lang (Berlin: Springer) p 59
[56] Vollmayr K, Reger J D, Scheucher M and Binder K 1993 *Z. Phys.* B **91** 113
[57] Stiefvater T, Müller K-R and Kühn R 1996 *Physica* A **232** 61
[58] Brangian C, Kob W and Binder K 2001 *Europhys. Lett.* **53** 756
[59] Suzuki M 1977 *Prog. Theor. Phys.* **58** 1142
[60] Hohenberg P C and Halperin B I 1977 *Rev. Mod. Phys.* **49** 435
[61] Bhatt R N and Young A P 1992 *Europhys. Lett.* **20** 59
[62] Jayaprakash C, Chalupa J and Wortis M 1977 *Phys. Rev.* B **15** 1495
[63] Mackenzie N D and Young A P 1983 *J. Phys. C: Solid State Phys.* **16** 5321
[64] Billoire A and Marinari E 2001 *Preprint* cond-mat/0101177
[65] Horbach J and Kob W 1999 *Phys. Rev.* B **60** 3169
[66] Glotzer S C, Jan N and Poole P H 1998 *Phys. Rev.* E **57** 7350
[67] Kondor I 1989 *J. Phys. A: Math. Gen.* **22** L163
[68] Ritort F 1994 *Phys. Rev.* B **50** 6844
[69] Kim K and Yamamoto R 2000 *Phys. Rev.* E **61** R41
[70] Biroli G and Monasson R 2000 *Europhys. Lett.* **50** 155
[71] Parisi G, Ritort F and Slanina F 1998 *J. Phys. A: Math. Gen.* **26** 247
Parisi G, Ritort F and Slanina F 1998 *J. Phys. A: Math. Gen.* **26** 3775
[72] Ricci-Tersenghi F and Zecchina R 2000 *Phys. Rev.* E **62** R7567
[73] Barrat A and Zecchina R 1999 *Phys. Rev.* E **59** R1299
[74] Franz S, Donati C, Parisi G and Glotzer S C 1999 *Phil. Mag* B **79** 1827
[75] Franz S and Parisi G 2000 *J. Phys.: Condens. Matter* **12** 6335
[76] Brangian C, Kob W and Binder K 2002 in preparation
[77] Picco M, Ritort F and Sales M 2001 *Eur. Phys. J.* B **19** 565